miRNA-21 promotes the progression of acute liver failure via the KLF6/autophagy/IL-23 signaling pathway

SUXIA BAO[1*], WEIYANG ZHENG[2*], RONG YAN[3] and JIE XU[1]

[1]Department of Infectious Disease, Shanghai Ninth People's Hospital; [2]Department of Infectious Disease, Xinhua Hospital, Shanghai Jiao Tong University School of Medicine, Shanghai 200011; [3]Department of Infectious Diseases, Zhejiang Provincial People's Hospital, People's Hospital of Hangzhou Medical College, Hangzhou, Zhejiang 310014, P.R. China

Received May 11, 2023; Accepted January 10, 2024

DOI: 10.3892/mmr.2024.13205

Abstract. Acute liver failure (ALF) is a complex syndrome characterized by overactivation of innate immunity, and the recruitment and differentiation of immune cells at inflammatory sites. The present study aimed to explore the role of microRNA (miRNA/miR)-21 and its potential mechanisms underlying inflammatory responses in ALF. Baseline serum miR-21 was analyzed in patients with ALF and healthy controls. In addition, miR-21 antagomir was injected via the tail vein into C57BL/6 mice, and lipopolysaccharide/D-galactosamine (LPS/GalN) was injected into mice after 48 h. The expression levels of miR-21, Krüppel-like-factor-6 (KLF6), autophagy-related proteins and interleukin (IL)-23, and hepatic pathology were then assessed in the liver tissue. Furthermore, THP-1-derived macrophages were transfected with a miRNA negative control, miR-21 inhibitor, miR-21 mimics or KLF6 overexpression plasmid, followed by treatment with or without rapamycin, and the expression levels of miR-21, KLF6, autophagy-related proteins and IL-23 were evaluated. The results revealed that baseline serum miR-21 levels were significantly upregulated in patients with ALF. In addition, LPS/GalN-induced ALF was attenuated in the antagomir-21 mouse group. KLF6 was identified as a target of miR-21-5p with one putative seed match site identified by TargetScan. A subsequent luciferase activity assay demonstrated a direct interaction between miR-21-5p and the 3'-UTR of KLF6 mRNA. Further experiments suggested that miR-21 promoted the expression of IL-23 via inhibiting KLF6, which regulated autophagy. In conclusion, in the present study, baseline serum miR-21 levels were highly upregulated in patients with ALF, antagomir-21 attenuated LPS/GalN-induced ALF in a mouse model, and miR-21 could promote the expression of IL-23 via inhibiting KLF6.

Correspondence to: Professor Jie Xu, Department of Infectious Disease, Shanghai Ninth People's Hospital, Shanghai Jiao Tong University School of Medicine, 280 Mohe Road, Shanghai 200011, P.R. China
E-mail: dr.xu@aliyun.com

*Contributed equally

Key words: acute liver failure, microRNA-21, macrophage, autophagy, interleukin-23

Introduction

Acute liver failure (ALF) is a complex syndrome characterized by overactivation of innate immunity, and the recruitment and differentiation of immune cells at the inflammatory site, which plays important roles in inducing liver injury (1). Our previous study suggested that baseline serum interleukin (IL)-23 levels were highly increased, and that upregulated baseline IL-23 levels were associated with mortality in patients with liver failure (2). However, to the best of our knowledge, few related mechanistic studies have been performed (2,3).

MicroRNAs (miRNAs/miRs) are noncoding RNAs composed of 19-22 nucleotides that regulate gene expression at the post-transcriptional level by inducing degradation of mRNA or inhibiting its transcription (4). A previous miRNA microarray analysis demonstrated that miR-21 is increased in patients with sepsis (5); however, to the best of our knowledge, the role of miR-21 in ALF has not been elucidated. Therefore, the present study explored the role of miR-21 and its potential mechanisms in the inflammatory responses of patients with ALF.

Krüppel-like-factor-6 (KLF6) is a widely expressed nuclear transcriptional regulator, which has been considered a tumor suppressor gene, and regulator of cell proliferation, tumorigenesis, differentiation and signal transduction (6). The KLF family constitutes zinc finger proteins that have a conserved zinc finger DNA-binding domain, which can bind to GC-rich motifs on various target genes. KLF6 can act as both a repressor and an activator of transcription (7). A previous study demonstrated that KLF6 alleviates hepatic ischemia-reperfusion injury by inhibiting autophagy (8). By contrast, another study suggested that KLF6 is a transcriptional activator of autophagy in acute liver injury (9). However, whether and how KLF6 plays a role in ALF remain unknown.

Accumulating evidence has demonstrated that autophagy serves a crucial role in ischemia-reperfusion injury of the liver, lung, heart, kidney and brain (10). Numerous studies on ischemia-reperfusion injury in the liver, heart and brain

have corroborated this perspective (9,11-15). The regulation of autophagy is significantly influenced by the KLF family. Notably, conserved KLFs/autophagy pathways have been reported to regulate the lifespan of nematodes and mammalian age-related vascular deterioration (16). In addition, the communication between autophagy and KLF2 in acute liver injury determines the endothelial phenotype and microvascular function (17). However, the effects and underlying mechanism of KLF6 on autophagy in ALF are unknown. The present study aimed to explore the role of miR-21 and its potential mechanisms underlying inflammatory responses in ALF.

Materials and methods

Patients. From June 2015 to July 2017, a total of 66 patients participated in the present study, including 40 patients with ALF and 26 healthy controls (HCs). The median age of the study subjects was 42 years (age range: 15-82 years) and 72.73% of patients were male. Enrolled patients were treated in accordance with the scheduled criteria (18), and the inclusion criteria were as follows: An illness duration of <26 weeks in a patient without preexisting liver disease or cirrhosis associated with any degree of mental status alteration (encephalopathy) and coagulopathy (an international normalized ratio ≥1.5). The exclusion criteria were as follows: i) Liver transplant; ii) the presence of any concomitant illness; and iii) the use of liver support devices. All enrolled participants were hospitalized and followed-up at the Zhejiang Provincial People's Hospital, People's Hospital of Hangzhou Medical College (Hangzhou, China). Written informed consent was obtained from subjects prior to participation. The study was performed according to the Ethical Principles for Medical Research Involving Human Subjects outlined in The Helsinki Declaration in 1975, and the research was approved by the Ethics Committee of Zhejiang Provincial People's Hospital, People's Hospital of Hangzhou Medical College (approval no. ZRY-T123-59).

Construction of the animal model. A total of 21 C57BL/6 male mice (age, 6-8 weeks; weight, 18-22 g), which were randomly divided into three groups (n=7 mice/group), were obtained from the Experimental Animal Center of the Chinese Academy of Sciences. All mice were raised at a room temperature of 22±2˚C and 55±5% relative humidity, with free access to food and water. Mice were acclimated to the environment for 6-7 days under a 12-h dark/light cycle.

The combination of LPS/GalN (MilliporeSigma) was dissolved and injected intraperitoneally (400 mg/kg GalN and 10 μg/kg LPS). To assess the role of miR-21 in LPS/GalN-induced ALF, mice were challenged with a tail vein injection of 20 nmol miRNA antagomir negative control (NC) or 20 nmol miR-21 antagomir (both from Shanghai GenePharma Co., Ltd.). The mice were then challenged intraperitoneally with 10 μg/kg LPS and 400 mg/kg GalN, or phosphate-buffered saline (PBS; control), after 48 h. Mice were sacrificed if they exhibited listlessness, respiratory abnormalities, loss of appetite, weight loss (maximum 20%) and disordered mobility. Otherwise, the mice were sacrificed 24 h after LPS/GalN injection. Mice were euthanized by cervical dislocation following anesthesia with an intraperitoneal injection of sodium pentobarbital (35 mg/kg). All procedures were conducted in accordance with the guide for the care and use of laboratory animals (19) and the study was approved by the Ethics Committee of Zhejiang Provincial People's Hospital, People's Hospital of Hangzhou Medical College (approval no. 20190010).

Cell culture. THP-1 cells were purchased from Pricella Life Science & Technology Co., Ltd. The cells ($3x10^5$ cells/well) were cultured in 6-well plates in RPMI-1640 (cat. no. 11875119; Gibco; Thermo Fisher Scientific, Inc.) containing 10% heat-inactivated fetal calf serum (cat. no. 12484028; Gibco; Thermo Fisher Scientific, Inc.) and 1% penicillin-streptomycin (Hyclone; Cytiva) at 37˚C in a 5% CO_2 incubator. To obtain THP-1-derived macrophages, THP-1 cells were then treated with 160 ng/ml phorbol 12-myristate 13-acetate (PMA; cat. no. P8139; MilliporeSigma) followed by 24 h of incubation at 37˚C in a 5% CO_2 incubator in RPMI-1640 to obtain M0 macrophages. The macrophages were polarized to M1 macrophages by incubation with 10 pg/ml LPS (MilliporeSigma) and 20 ng/ml IFN-γ (R&D Systems, Inc.) for 18 h at 37˚C in a 5% CO_2 incubator. Then, the THP-1-derived macrophages were maintained in fresh RPMI-1640.

RNA extraction, and quantification of mRNA and miRNA expression. Total miRNA was extracted and purified from 150 μl mouse human plasma, which was obtained by centrifuging blood samples at 2,000 x g at 4˚C for 10 min using the miRNeasy Serum/Plasma Kit (cat. no. 217184; Qiagen GmbH) according to the manufacturer's instructions. The quality and concentration were assessed using a NanoDrop 2000 spectrophotometer (Thermo Fisher Scientific, Inc.) based on the ratio of absorbance at 260 nm. The purified miRNA was immediately reverse-transcribed using the miScript II Reverse Transcription Kit (Qiagen GmbH) according to the manufacturer's instructions. The expression levels of serum miR-21 were quantified using an Applied Biosystems 7500 real-time PCR system (Applied Biosystems; Thermo Fisher Scientific, Inc.). qPCR was performed using miScript SYBR Green PCR Kit with primers specific for miR-21 (all from QIAGEN GmbH) according to the manufacturer's instructions. The thermocycling protocol was: 15 min at 95˚C, followed by 40 cycles at 94˚C for 15 sec, 55˚C for 30 sec and 70˚C for 30 sec. The primer sequences are listed in Table I.

Total RNA was extracted from THP-1-derived macrophages and from mouse liver tissues, which were collected when mice were sacrificed, using TRIzol® reagent (Invitrogen; Thermo Fisher Scientific, Inc.). The quality and concentration of RNA were assessed using a NanoDrop 2000 spectrophotometer based on the ratio of absorbance at 260 nm. A PrimeScript ™ RT Reagent kit (Takara Bio, Inc.) was used to reverse transcribe 2 μg RNA into cDNA using the following protocol: 25˚C for 5 min, 42˚C for 30 min and 85˚C for 5 min, followed by maintenance at 4˚C for 5 min. Amplification of the cDNA was performed by qPCR using a SYBR Premix Ex Taq™ II kit (Takara Bio, Inc.). The thermocycling protocol was: 95˚C for 3 min, followed by 40 cycles of denaturation at 95˚C for 30 sec, annealing at 60˚C for 30 sec and extension at 72˚C for 1 min, and a final extension step at 72˚C for 7 min. The primer sequences are listed in Table I. The relative expression levels of mRNA and miRNA were calculated using the $2^{-\Delta\Delta Cq}$

Table I. Primers for quantitative PCR analysis.

Gene	Forward primer, 5'-3'	Reverse primer, 5'-3'
H-miR-21	TGCGGCTAGCTTATCAGACT	Universal primer: GTGCAGGGTCCGAGGT
H-U6	CTCGCTTCGGCAGCACA	AACGCTTCACGAATTTGCGT
H-KLF6	CAAGGGAAATGGCGATGCCT	CTTTTCTCCTGTGTGCGTCC
H-IL-23	GCTTCAAAATCCTTCGCAG	TATCTGAGTGCCATCCTTGAG
GAPDH	AGGCCGGATGTGTTCGC	CAAATCCGTTGACTCCGACC
m-miR-21	TGCGGCTAGCTTATCAGACTGA	Universal primer: GTGCAGGGTCCGAGGT
m-U6	CTCGCTTCGGCAGCACA	AACGCTTCACGAATTTGCGT

H, human; IL, interleukin; KLF6, Krüppel-like-factor-6; m, murine; miR, microRNA.

method (20). GAPDH was used as an endogenous control for mRNA expression and U6 was used as an endogenous control for miRNA expression. The specificity of the products was verified using melting curve analysis.

Western blot analysis and antibodies. Total protein was extracted from mouse liver tissue and THP-1-derived macrophages using RIPA lysis buffer (Beyotime Institute of Biotechnology) and proteins were quantified using a bicinchoninic acid protein assay kit (cat. no. P0012S; Beyotime Institute of Biotechnology). An equal amount of protein (50 μg/lane) was separated by SDS on 12% gels and was then transferred to a nitrocellulose blotting membrane. The membranes were blocked with 5% non-fat milk dissolved in TBS-0.1% Tween buffer for 2 h at room temperature and were then probed with the following primary antibodies: IL-23 (1:1,000; cat. no. ab190356; Abcam), KLF6 (1:1,000; cat. no. DF13114; Affinity Biosciences), LC3A/B (1:1,000; cat.no. ab62721; Abcam), p62 (1:1,000; cat. no. ab155686; Abcam), ATG7 (1:1,000; cat. no. ab133528; Abcam), Beclin1 (1:1,000; cat. no. ab207612; Abcam) and GAPDH (1:2,500; cat. no. ab9485; Abcam). The membranes were then incubated with HRP-conjugated anti-mouse or anti-rabbit secondary antibodies (1:2,000; cat. nos. ab6789 and ab6721; Abcam) for 2 h at room temperature. Signals were visualized using enhanced chemiluminescence reagent (Thermo Fisher Scientific, Inc.) according to the manufacturer's instructions. Densitometric analysis was performed using ImageJ (Version 1.49; National Institutes of Health).

Histological changes in mouse livers. Liver sections collected from mice after sacrifice were fixed with 10% neutral-buffered formalin for 36 h at room temperature, embedded in paraffin and cut into 5-μm slices. After deparaffinization and rehydration, the slices were stained with 1% hematoxylin for 10 min and 0.5% eosin for 3 min at room temperature. Histological changes were evaluated using a light microscope by two experienced pathologists.

ELISA. Plasma was obtained by centrifuging mouse blood samples at 2,000 x g for 10 min at 4˚C and was then stored at -80˚C. Alanine transaminase (ALT; cat. no. C009-2; Nanjing Jiancheng Bioengineering Institute), aspartate transaminase (AST; cat. no. C010-2; Nanjing Jiancheng Bioengineering Institute) and IL-23 (cat. no. BMS6017TEN; Invitrogen; Thermo Fisher Scientific, Inc.) kits were used to assess the levels of ALT, AST and IL-23, according to the manufacturers' protocols. The signal was measured at 450 nm excitation using a SpectraMax® i3 multifunctional microplate reader (Molecular Devices, LLC). After the standard curve was established, the plasma levels were calculated based on the absorbance values of each sample.

Cell transfection. The miR-21 mimics (sense: 5'-UAGCUU AUCAGACUGAUGUUGA-3'; antisense: 5'-AACAUC AGUCUGAUAAGCUAUU-3'), miR-21 inhibitor (5'-UCA ACAUCAGUCUGAUAAGCUA-3'), miR-21 mimics negative control (NC) (sense: 5'-UUCUCCGAACGUGUCACG UTT-3'; antisense: 5'-ACGUGACACGUUCGGAGAATT-3') and miR-21 inhibitor NC (5'-CAGUACUUUUGUGUAGUA CAA-3') were purchased from Guangzhou RiboBio Co., Ltd. THP-1-derived macrophages ($3x10^5$ cells/well) were inoculated in 6-well plates and the transfection experiment was started when the cell confluence reached 70%. During transfection, 12 μl Lipofectamine® 2000 (Invitrogen; Thermo Fisher Scientific, Inc.) was added to 150 μl serum-free opti-MEM (cat. no. 31985070; Gibco; Thermo Fisher Scientific, Inc.) and mixed with 10 μl miR-21 mimics/inhibitors, then maintained at room temperature for 20 min. The final concentration of miR-21 mimics and miR-21 mimics NC was 50 nM, and the final concentration of the miR-21 inhibitor and miR-21 inhibitor NC was 100 nM. After 20 min at room temperature, the mixed solution was added to the 6-well plates to complete the transfection and incubated for 6 h at 37˚C in a 5% CO_2 incubator. Then, the medium was replaced with RPMI-1640 containing 10% heat-inactivated fetal calf serum and 1% penicillin-streptomycin. The cells were then incubated for 48 h at 37˚C in a 5% CO_2 incubator.

In addition, THP-1-derived macrophages ($3x10^5$ cells/well) were cultured with 5 μM rapamycin (cat. no. 53123-88-9; MedChemExpress), which is an autophagy inducer. After incubation for 1 h at 37˚C in a 5% CO_2 incubator, THP-1-derived macrophages were transfected with miR-21 mimics or miR-21 mimics NC using Lipofectamine 2000 for 6 h at 37˚C in a 5% CO_2 incubator. Then, the medium was replaced with RPMI-1640 containing 10% heat-inactivated fetal calf serum and 1% penicillin-streptomycin and incubated for 48 h at 37˚C in a 5% CO_2 incubator.

Furthermore, 1 μg KLF6 overexpression plasmid (cat. no. HG12365-ACG; Sino Biological, Inc.), with the pCMV3 backbone, 1 μg pCMV3-C-GFPSpark control vector (cat. no. CV026; Sino Biological, Inc.), 50 nM miR-21 mimics NC and 50 nM miR-21 mimics were transfected into THP-1-derived macrophages using Lipofectamine 2000 for 6 h at 37˚C in a 5% CO_2 incubator. Then, the medium was replaced with RPMI-1640 containing 10% heat-inactivated fetal calf serum and 1% penicillin-streptomycin and incubated for 48 h at 37˚C in a 5% CO_2 incubator.

Analysis of target genes of miRNA using TargetScan. Target genes of miR-21 were evaluated using TargetScan 8.0 software (https://www.targetscan.org/vert_80/).

Luciferase activity assay. For the luciferase assay, the KLF6-expression construct was generated using a full-length of clone KLF6, which was inserted into psiCHECK™-2 Vector (cat. no. C8021; Promega Corporation). The miR-21-5p binding site found in the 3'-UTR of the KLF6 mRNA using TargetScan 8.0 software, and its mutated version, were cloned into a modified pGL3-control vector (cat. no. E1741; Promega Corporation). Subsequently, 293T cells (cat. no. CL-0005; Procell Life Science & Technology Co., Ltd.) were cotransfected with reporter constructs containing wild-type (WT) or mutant (MUT) KLF6 3'-UTR and miR-21-5p mimics (50 nM) or miR-21 mimics NC (50 nM) using Lipofectamine 2000. Then, 293T cells were harvested and lysed 48 h after transfection. Luciferase reporter activities were evaluated using the Dual-Glo Luciferase Assay System (Promega Corporation). Firefly luciferase activity was standardized to *Renilla* luciferase activity.

GFP-LC3 analyses. After cotransfection of THP-1-derived macrophages with miR-21 mimics or miR-21 mimics NC and 1.5 μg pCMV-GFP-LC3B (cat. no. D2815; Beyotime Institute of Biotechnology) using Lipofectamine 2000 for 6 h at 37˚C in a 5% CO_2 incubator. Then, the medium was replaced with RPMI-1640 containing 10% heat-inactivated fetal calf serum and 1% penicillin-streptomycin and incubated for 24 h at 37˚C in a 5% CO_2 incubator. Nuclei were stained with DAPI for 20 min at 4˚C in the dark. Images of GFP-LC3 puncta were captured under a confocal fluorescence microscope (Leica Microsystems, Inc.).

Statistical analysis. All data were assessed using GraphPad 5.0 (Dotmatics) and SPSS 19.0 (IBM Corp.). Results are presented as the mean ± standard deviation. Comparisons between two groups were carried out via paired Student's t-test or unpaired Student's t-tests. Multiple comparisons were carried out via homogeneity test of variance followed by one-way ANOVA and Tukey's post hoc test. Two-tailed $P \leq 0.05$ was considered to indicate a statistically significant difference. Each *in vitro* experiment was repeated three times.

Results

Serum miR-21 levels are significantly increased in patients with ALF. Serum miR-21 levels, detected by qPCR, were compared between the HC and ALF groups (Fig. 1A), and the results suggested that the serum levels of miR-21 were significantly higher in the ALF group than those in the HC group. Moreover, serum miR-21 levels were highly upregulated in 13 non-surviving patients with ALF compared with those in the 27 surviving patients with ALF (Fig. 1B). To explore the role of miR-21 in patients with ALF, serum miR-21 levels were evaluated before and after treatment in 27 surviving and 13 non-surviving patients with ALF before and after treatment (Fig. 1C and D). The results demonstrated that serum miR-21 levels were markedly decreased in the surviving group of patients with ALF after treatment. However, there was no statistically significant difference in serum miR-21 levels before and after treatment in non-surviving patients with ALF.

LPS/GalN-induced ALF is attenuated in antagomir-21-treated mice. To further explore the role of miR-21 in the pathogenesis of ALF, the effects of miR-21 antagomir were evaluated in an LPS/GalN-induced male mouse model of ALF, which has a more stable physical condition with fewer individual differences compared with a female mouse model of ALF, similar to the liver failure model we have previously constructed (3). Briefly, following treatments, serum was isolated and liver tissues were collected. The expression levels of miR-21 in the liver tissues were evaluated by qPCR (Fig. 2A). The results demonstrated that the expression levels of miR-21 were significantly increased in the LPS/GalN-induced ALF mouse model compared with in the PBS control group. However, the injection of antagomir-21 blocked the upregulation of miR-21, demonstrating that a mouse model of LPS/GalN-induced ALF with miR-21 inhibition was successfully constructed. To explore the role of miR-21 in the LPS/GalN-induced ALF mouse model, the present study further explored liver function and pathological damage to the liver. As shown in Fig. 2B, ALT and AST levels in the LPS/GalN group were significantly increased, whereas they were decreased in the antagomir-21 ALF mouse group. Similarly, the degree of liver damage, including disordered structure of liver lobules, increased infiltration of inflammatory cells (blue arrow), hyperchromatic nuclei, hypochromatosis and appearance of necrosis (red arrow), in the LPS/GalN-induced ALF mouse model was markedly aggravated, whereas the degree of the aforementioned liver damage was relieved in the antagomir-21 LPS/GalN mouse group (Fig. 2C). These results suggested that LPS/GalN-induced ALF is attenuated by antagomir-21.

To further evaluate the potential mechanisms of miR-21, KLF6 (GenBank accession number: NM_001300.6) was considered a target of miR-21, with one putative miR-21-5p seed match site determined using the TargetScan database (Fig. 2D). Therefore, the expression levels of KLF6 were assessed, and the results demonstrated that the protein expression levels of KLF6 were markedly decreased in the LPS/GalN group compared with those in the PBS control group. By contrast, the decreased expression of KLF6 protein in the LPS/GalN-induced ALF mouse model was abrogated in the antagomir-21 mouse group (Fig. 2E).

Furthermore, the levels of IL-23 were detected in the antagomir-21 mouse model. The results demonstrated that serum IL-23 was significantly suppressed in the antagomir-21 ALF mouse group compared with that in the miRNA antagomir NC ALF mouse group, as detected by ELISA

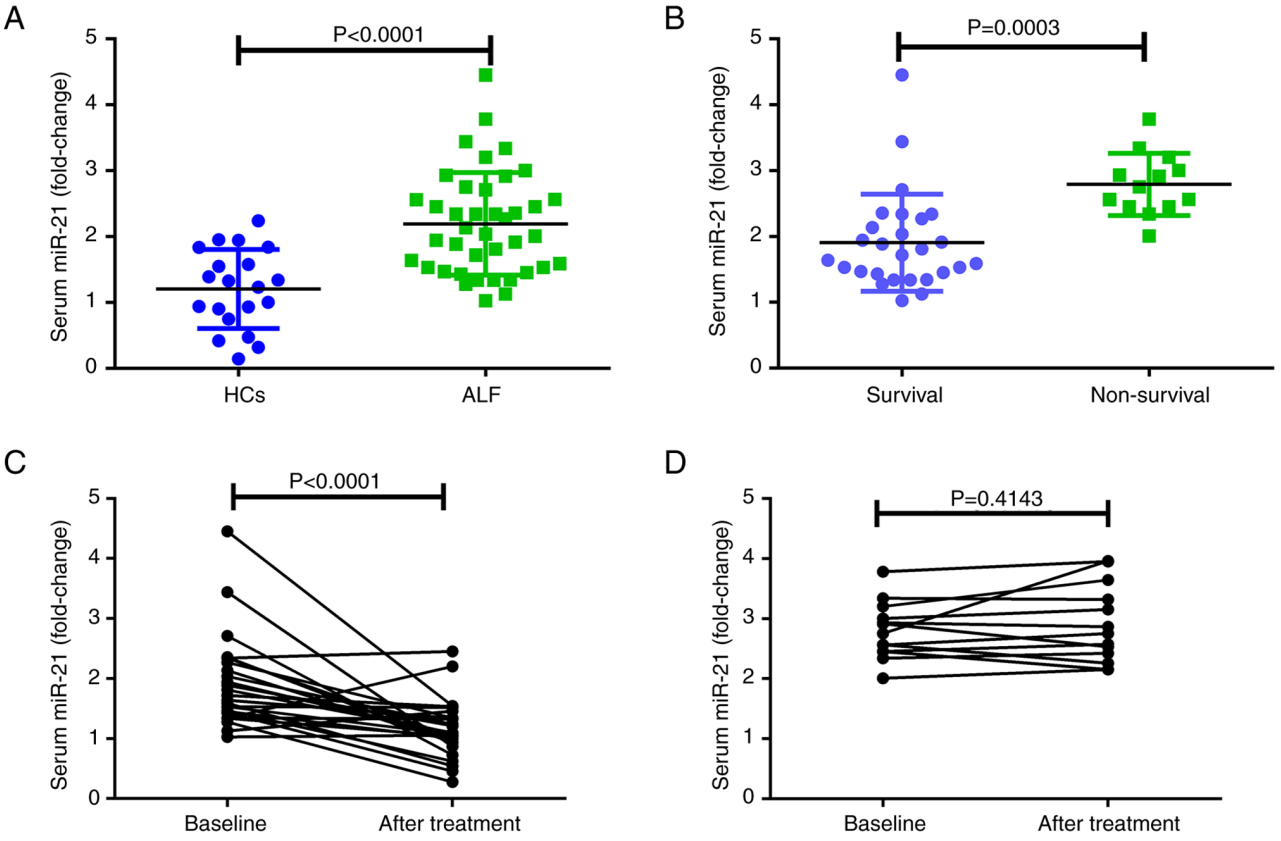

Figure 1. Serum miR-21 levels are significantly upregulated in patients with ALF. (A) Baseline expression levels of serum miR-21 from patients with ALF and HCs, as measured by quantitative PCR. (B) Baseline expression levels of serum miR-21 were further analyzed in non-surviving and surviving patients with ALF. Serum miR-21 expression levels were evaluated at baseline and after treatment in the (C) survival group and (D) non-survival group of patients with ALF. ALF, acute liver failure; HCs, healthy controls; miR, microRNA.

(Fig. 2F). As shown in Fig. 2G, the protein expression levels of IL-23 in the liver tissues exhibited the same trend, as determined by western blotting. These results indicated that miR-21 may promote the expression of IL-23.

Moreover, the levels of autophagy markers were explored in the antagomir-21 mouse model. The results demonstrated that the LC3II/I ratio was upregulated and the protein expression levels of p62 were reduced in the antagomir-21 ALF mouse group compared with those in the miRNA NC ALF mouse group (Fig. 2H). These results demonstrated that miR-21 could inhibit autophagy.

miR-21 promotes the expression of IL-23 and inhibits the expression of KLF6. To explore the underlying mechanisms of miR-21, the miR-21 inhibitor, miRNA inhibitor NC, miR-21 mimics and miR-21 mimics NC were used to interfere with the expression levels of miR-21 in THP-1-derived macrophages, which was confirmed by qPCR. As shown in Fig. 3A, the transfection efficiency of the miR-21 inhibitor and miR-21 mimics were confirmed by qPCR. The relative expression levels of miR-21 were significantly upregulated in the miR-21 mimics group compared with those in the miR-21 mimics NC group, and the relative expression levels of miR-21 were significantly decreased in the miR-21 inhibitor group compared with those in the miRNA inhibitor NC group. Therefore, the miR-21 mimics and miR-21 inhibitor were used for subsequent overexpression and knockdown experiments.

Our previous study suggested that IL-23 was highly increased in patients with ALF (3). To explore whether a relationship exists between miR-21 and IL-23 in THP-1-derived macrophages, the expression levels of IL-23 were explored in the miR-21 overexpression and knockdown groups. The results demonstrated that IL-23 expression was significantly increased in the miR-21 mimics group compared with that in the miR-21 mimics NC group, whereas IL-23 expression was significantly suppressed in the miR-21 inhibitor group compared with that in the miRNA inhibitor NC group, as detected by western blotting (Fig. 3B). As shown in Fig. 3C, the levels of IL-23 in the cell supernatants exhibited the same trend, as determined by ELISA. These results indicated that miR-21 promoted the expression of IL-23.

KLF6 was identified as a target gene of miR-21, with one putative miR-21-5p seed match site (KLF6 3'-UTR 724-730), using the TargetScan database. To explore whether miR-21-5p directly targets the KLF6 mRNA 3'-UTR (724-730 bp), reporter constructs (pGL3-KLF6) with putative WT or MUT 3'-UTR downstream of the firefly luciferase were cloned. 293T cells were cotransfected with pGL3-KLF6 and miR-21-5p mimics or miR-21 mimics NC. The results demonstrated that transfection with the miR-21-5p mimics resulted in a significant downregulation of the luciferase activity of the reporter plasmid containing the WT 3'-UTR; however, the downregulation of luciferase activity was fully abolished after point mutation in the miR-21-5p binding site in the 3'-UTR

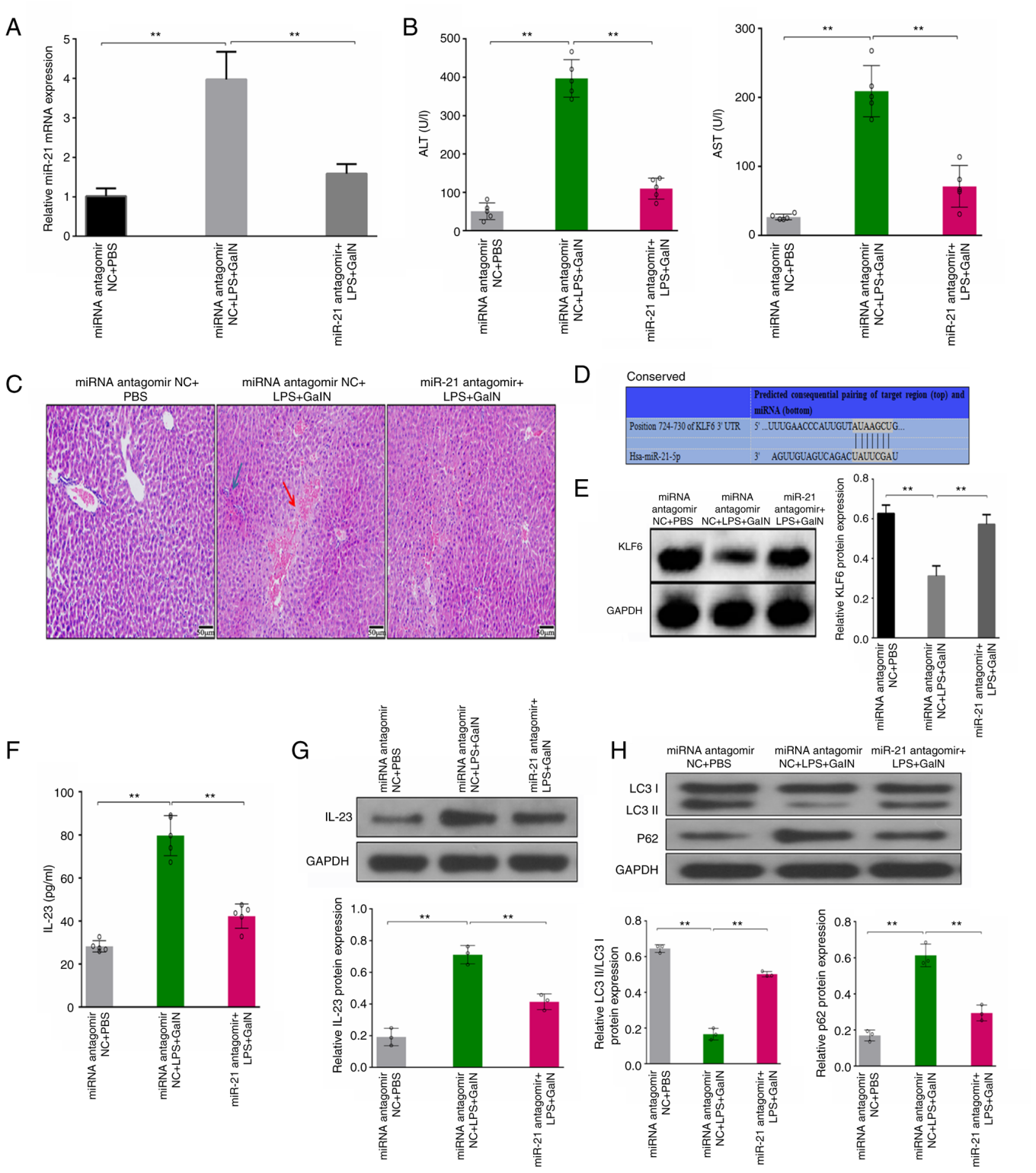

Figure 2. LPS/GalN-induced ALF is attenuated in antagomir-21-treated mice. (A) Relative expression levels of miR-21 in liver tissues from various groups were analyzed by quantitative PCR. (B) Serum ALT and AST levels were measured by ELISA in each group. (C) Representative photomicrographs of hematoxylin and eosin-stained sections of liver tissue from each group (magnification, x50). (D) TargetScan database demonstrated that KLF6 was a potential target of miR-21 with one putative miR-21-5p seed match site. (E) Protein expression levels of KLF6 were evaluated by western blotting of the liver tissues from each groups. (F) Serum IL-23 levels from various groups were measured by ELISA. Protein expression levels of (G) IL-23, and (H) LC3II/LC3I and p62 were evaluated by western blotting in liver tissues from various groups. **P<0.01. ALT, alanine transaminase; ALF, acute liver failure; AST, aspartate transaminase; GalN, D-galactosamine; IL, interleukin; LPS, lipopolysaccharide; miR, microRNA; NC, negative control.

of KLF6 (3'-UTR MUT) (Fig. 3D). These results indicated a direct interaction between miR-21-5p and the 3'-UTR of KLF6 mRNA.

To further confirm the bioinformatics-based predictions, THP-1-derived macrophages were transfected with miR-21 inhibitor or miR-21 mimics, and the mRNA and protein

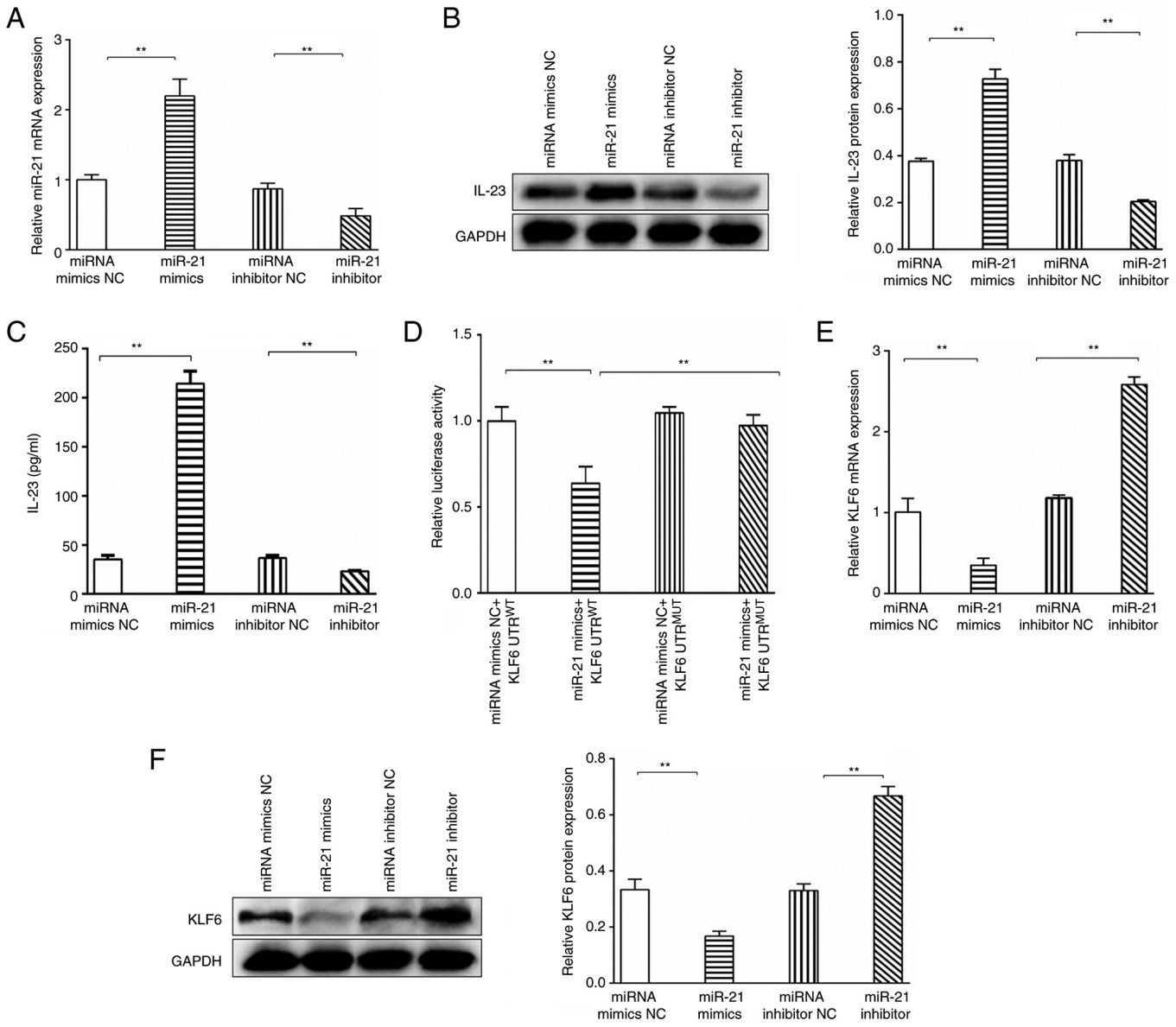

Figure 3. miR-21 promotes the expression of IL-23 and inhibits the expression of KLF6. (A) miR-21 mimics, miR-21 mimics NC, miR-21 inhibitor and miRNA inhibitor NC were constructed and transfected into THP-1-derived macrophages; the expression levels of miR-21 were confirmed by qPCR. (B) IL-23 protein expression levels were analyzed in THP-1-derived macrophages post-transfection by western blotting. (C) Levels of IL-23 in the cell supernatants were evaluated by ELISA. (D) Reporter constructs (pGL3-KLF6) with putative WT or MUT 3'-UTRs downstream of the firefly luciferase were cloned and cotransfected into cells with miR-21 mimics NC or miR-21 mimics, and relative luciferase activity was evaluated in the various groups. The relative expression levels of KLF6 were evaluated by (E) qPCR and (F) western blotting in various groups. **P<0.01. IL, interleukin; KLF6, Krüppel-like-factor-6; miR, microRNA; NC, negative control; MUT, mutant; ns, not significant; qPCR, quantitative PCR; WT, wild-type.

expression levels of KLF6 were evaluated by qPCR and western blotting, respectively. The relative expression levels of KLF6 were downregulated in the miR-21 mimics group compared with those in the miR-21 mimics NC group. However, introduction of the miR-21-5p inhibitor resulted in upregulation of the mRNA expression levels of KLF6 compared with those in the miRNA inhibitor NC group (Fig. 3E). As shown in Fig. 3F, KLF6 protein expression exhibited the same trend, as determined by western blotting. These results indicated that miR-21 inhibited the expression of KLF6.

miR-21 promotes the expression of IL-23 via inhibiting autophagy. It has been reported that 5-methoxytryptophan effectively alleviates liver cirrhosis by regulating FOXO3a/miR-21/ATG5 signaling pathway-mediated autophagy (21); therefore, it was hypothesized that miR-21 promoted the expression of IL-23 by impairing autophagy in patients with ALF. To experimentally verify this hypothesis, THP-1-derived macrophages were transfected with miR-21 mimics or miR-21 mimics NC. As expected, LC3I to LC3II conversion was highly upregulated and p62 protein expression was decreased in the miR-21 mimics NC group compared with those in the miR-21 mimics group, as determined by western blotting (Fig. 4A), which demonstrated that miR-21 inhibited autophagy. Consistently, overexpression of miR-21 highly suppressed GFP-LC3 puncta formation (Fig. 4B). Moreover, THP-1-derived macrophages were cultured with 5 μM rapamycin, which is an autophagy inducer. After 1 h, THP-1-derived macrophages

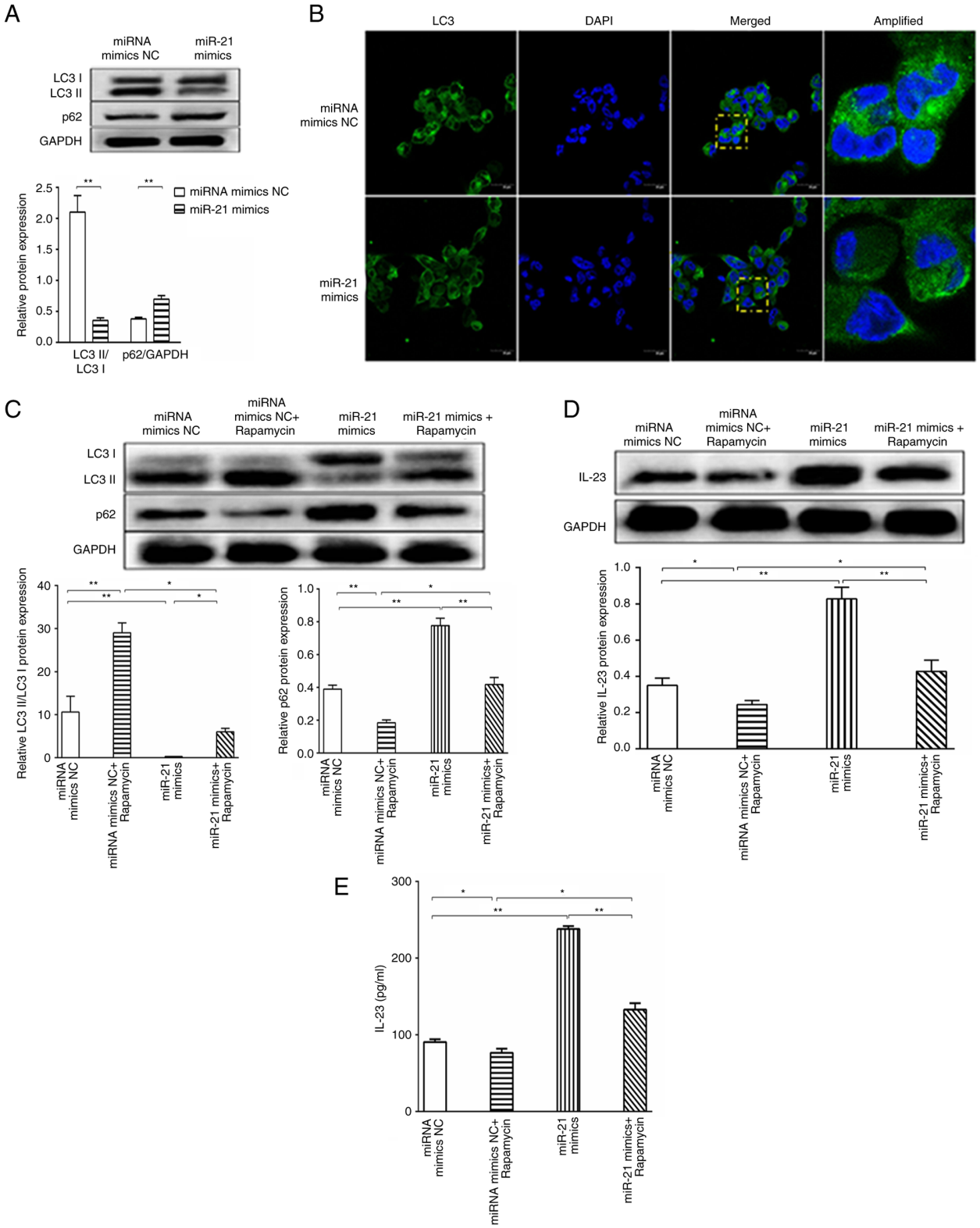

Figure 4. miR-21 promotes the expression of IL-23 via autophagy. (A) Western blot analysis of LC3II/I and p62 expression in macrophages transfected with miRNA mimics NC and miR-21 mimics. (B) Fluorescence images of LC3-GFP puncta formation in macrophages transfected with miRNA mimics NC or miR-21 mimics (magnification, x200 for the amplified images; magnification, x50 for the other images). (C) Western blot analysis of LC3II/I and p62 expression in macrophages transfected with miRNA mimics NC or miR-21 mimics and treated with rapamycin. (D) Western blot analysis of IL-23 expression in macrophages transfected with miRNA mimics NC or miR-21 mimics and treated with rapamycin. (E) IL-23 levels in the cell supernatant were analyzed post-transfection with miRNA mimics NC or miR-21 mimics and treated with rapamycin. *P<0.05, **P<0.01. IL, interleukin; miR, microRNA; NC, negative control.

were transfected with the miR-21 mimics or miR-21 mimics NC. The results demonstrated that the miRNA mimics NC + rapamycin group exhibited increased LC3I to LC3II conversion, decreased p62 protein expression (Fig. 4C) and

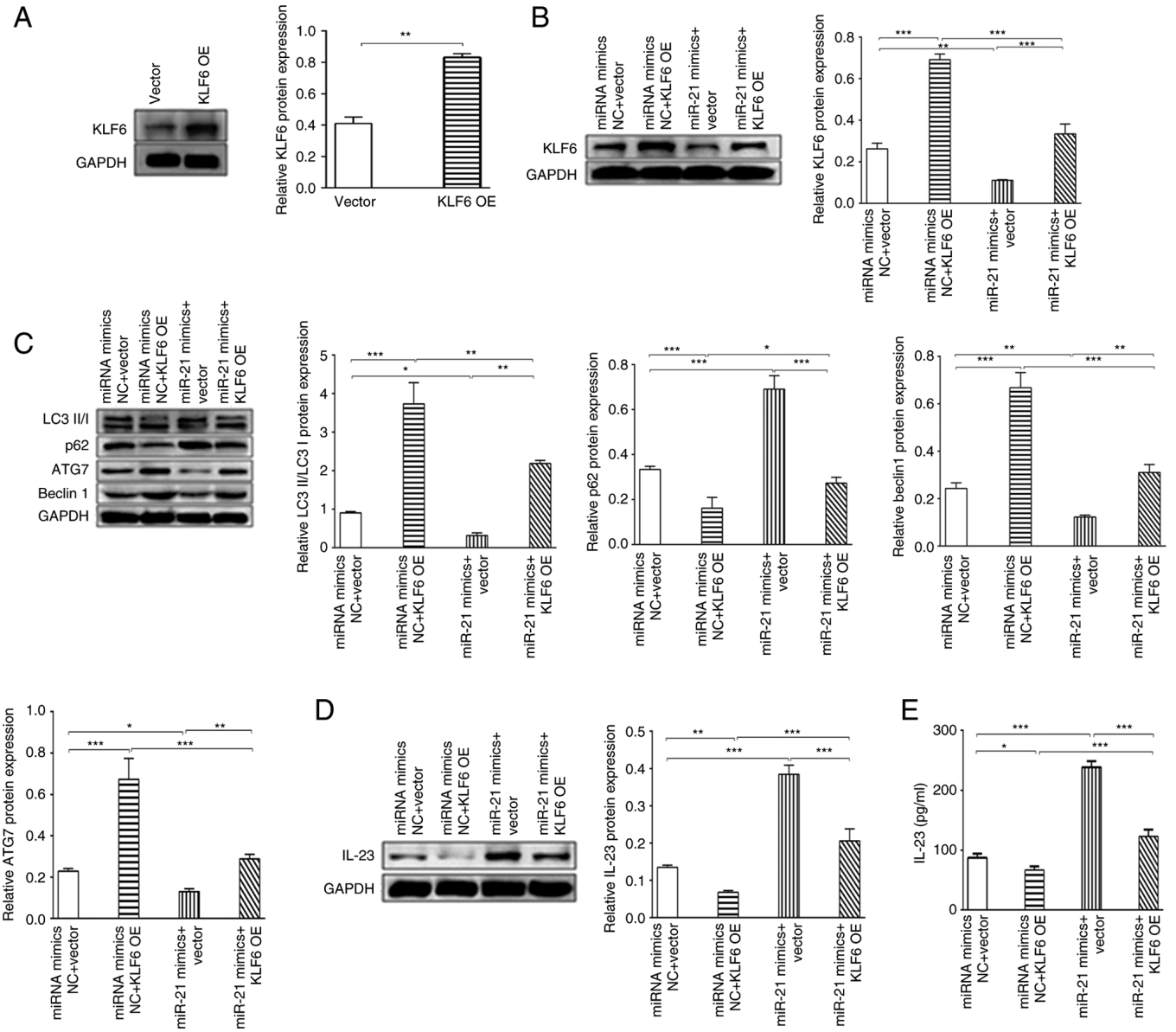

Figure 5. KLF6 promotes autophagy, and KLF6 blocks the miR-21-induced increase in IL-23 levels. (A) KLF6 OE plasmid and NC plasmid were transfected into THP-1-derived macrophages, and the expression levels of KLF6 were confirmed by western blotting. (B) Relative protein expression levels of KLF6 were evaluated by western blotting in THP-1-derived macrophages post-transfection. (C) Western blot analysis of LC3II/I, p62, ATG7 and Beclin 1 expression in macrophages post-transfection. (D) IL-23 expression was evaluated in THP-1-derived macrophages post-transfection.(E) ELISA evaluated the expression of IL-23 in the supernatant post-transfection. *P<0.05, **P<0.01, ***P<0.001. IL, interleukin; KLF6, Krüppel-like-factor-6; miR, microRNA; NC, negative control; OE, overexpression.

decreased IL-23 protein expression (Fig. 4D) compared with in the miRNA mimics NC group. In the miR-21 mimics group, LC3I to LC3II conversion was decreased, p62 protein expression was increased (Fig. 4C) and IL-23 protein expression was increased (Fig. 4D) compared with in the miRNA mimics NC group. Compared with in the miR-21 mimics group, the miR-21 mimics + rapamycin group exhibited increased LC3I to LC3II conversion, decreased p62 protein expression (Fig. 4C) and decreased IL-23 protein expression (Fig. 4D). Compared with in the miRNA mimics NC + rapamycin group, the miR-21 mimics + rapamycin group exhibited decreased LC3I to LC3II conversion, increased p62 protein expression (Fig. 4C) and increased IL-23 protein expression (Fig. 4D). Similarly, the cell supernatant levels of IL-23 exhibited the same trend, as determined by ELISA (Fig. 4E). In conclusion, these results demonstrated that miR-21 promoted the expression of IL-23 via inhibiting autophagy.

KLF6 promotes autophagy, and KLF6 blocks miR-21-induced increase in IL-23 levels. To explore the underlying mechanisms of KLF6, a KLF6 overexpression plasmid was used to induce the overexpression of KLF6, which was confirmed by western blotting. The KLF6 overexpression plasmid significantly increased the expression levels of KLF6 in THP-1-derived macrophages compared with the vector group (Fig. 5A), indicating that the KLF6 overexpression plasmid was successfully constructed. To explore whether the KLF6 overexpression plasmid inhibited the downregulation of KLF6 induced by miR-21, THP-1-derived macrophages were transfected with 50 nM miR-21 mimics or 50 nM miR-21 mimics NC, and 1 μg KLF6 overexpression plasmid or 1 μg

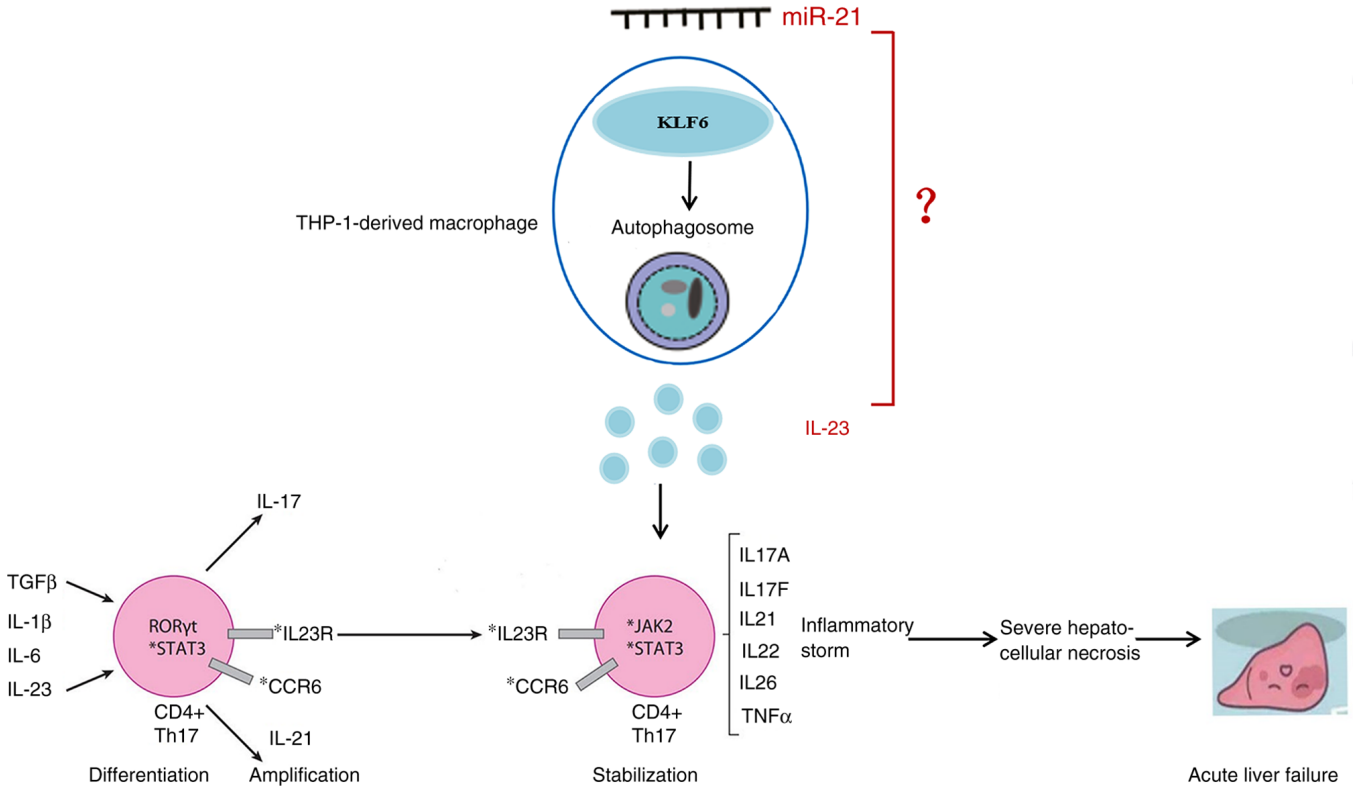

Figure 6. miR-21 promotes the expression of IL-23 via inhibiting KLF6, which promotes autophagy. miR-21 promoted the expression of IL-23 by targeting KLF6 in THP-1-derived macrophages, which regulates autophagy, thus promoting inflammatory storms, and subsequent severe hepatocellular necrosis and acute liver failure. IL, interleukin; KLF6, Krüppel-like-factor-6; miR, microRNA.

KLF6 control plasmid. The results demonstrated that miR-21 mimics could significantly inhibit KLF6 protein expression compared with miRNA mimics NC group, and KLF6 overexpression could significantly inhibit the downregulation of KLF6 expression induced by miR-21 mimics compared with the miR-21 mimics group (Fig. 5B).

The present study also evaluated whether KLF6 blocked the miR-21-induced decrease in autophagy levels. Compared with in the miRNA mimics NC group, overexpression of KLF6 could significantly upregulate the LC3II/I ratio, and the protein expression levels of Beclin1 and ATG7, and reduce the protein expression levels of p62 (Fig. 5C). Further study suggested that overexpression of KLF6 could upregulate miR-21-induced LC3II/I ratio, and the protein expression levels of Beclin1 and ATG7, and downregulate the protein expression levels of p62, which suggested that overexpression of KLF6 could block miR-21-induced downregulation of autophagy (Fig. 5C).

Moreover, the present study explored whether KLF6 blocked the miR-21-induced increase in IL-23 expression. The results suggested that overexpression of KLF6 could significantly reduce miR-21 mimics-induced IL-23 expression in THP-1-derived macrophages compared with miR-21 mimics group (Fig. 5D). The levels of IL-23 exhibited the same trend in the supernatant, as determined by ELISA (Fig. 5E). These results indicated that KLF6 blocked miR-21 induced-increases in IL-23 expression. In conclusion, miR-21 promoted the expression of IL-23 by inhibiting KLF6, which regulates autophagy, thus promoting inflammatory storms, and subsequent severe hepatocellular necrosis and ALF (Fig. 6).

Discussion

Although multiple miRNAs, including miR-21, have been found to be key regulators of liver regeneration (22,23), the potential mechanism in ALF is still incompletely understood. The present study demonstrated that serum miR-21 levels were significantly upregulated in patients with ALF. To explore the role of miR-21, a mouse model of ALF was constructed using LPS/GalN. The results suggested that the antagomir-21 treated mice alleviated LPS/GalN-induced ALF, as demonstrated by changes in liver function and liver pathology. Moreover, miR-21 promoted the expression of IL-23 via inhibiting KLF6, and KLF6 regulated autophagy. These results demonstrated that miR-21 may have a significant role in the pathogenesis of LPS/GalN-induced ALF and that blocking the expression of miR-21 could alleviate the degree of ALF.

miRNAs regulate gene expression at the post-transcriptional level by inhibiting transcription or inducing degradation of mRNA (24). However, the role of miR-21 in ALF has not been completely elucidated. Previous research has demonstrated that miR-21 contributes to ALF in septic mice by inhibiting PPARα expression (25). The overexpression of miR-21 has been shown to promote hepatocyte proliferation and liver regeneration by targeting PTEN, thus suggesting that increased miR-21 may be a treatment strategy to promote liver regeneration (26). miR-21 might also be considered a potential biomarker for the development and progression of sepsis, which could predict the prognosis of patients with sepsis (27). Another study has demonstrated that dysregulation of miR-21 may explain the abnormal inflammation and

persistent M1 macrophage polarization seen in diabetic wounds (28). The present study indicated that serum miR-21 levels were increased in patients with ALF, and this result was further verified in LPS/GalN-induced ALF mouse model. The injection of antagomir-21, which negatively regulates miR-21 expression, alleviated LPS/GalN-induced ALF, as demonstrated by pathological changes in the liver.

Autophagy is a ubiquitous homeostatic mechanism in eukaryotic cells that serves an important role in maintaining cell differentiation, development, homeostasis and survival (29). Autophagy is maintained at a low level to regulate cellular homeostasis, such as protein or organelle turnover, under normal physiological conditions (30). When the external environment changes, such as in response to a lack of nutrients or stress, autophagy can help cells survive (31). Studies have shown that certain cytokines, such as IL-6 and IL-8, can regulate the production of autophagy, and autophagy can also regulate the secretion of cytokines, such as IL-1β and IL-10 (32-34). The present study demonstrated that autophagy was significantly downregulated in LPS/GalN-induced liver injury.

The diverse roles of the KLF family in regulating autophagy have previously been reported. KLF15 transcriptionally activates ATG14 to promote autophagy and attenuate damage of oxidized low density lipoprotein-induced human aortic endothelial cells (35). KLF4 strengthens the sensitivity of colon cancer cells to 5-fluorouracil by targeting RAB26 to restrain autophagy (36). KLF2 critically regulates the neurogenesis of dental pulp-derived stem cells by inducing mitophagy and autophagy (37). The present study demonstrated that KLF6 promoted autophagy, and KLF6 blocks miR-21-induced increases in IL-23 expression.

The mobilization and differentiation of immune cells in the inflammatory site is caused and enhanced by inflammatory cytokines, such as IL-6, IL-17 and IL-23, which serve key roles in causing ALF (18). Antigen-presenting cells, including macrophages, are important modulators of immunity, and are important in adjusting innate and adaptive immune responses (38). A previous study suggested that KLF6 can promote inflammatory and hypoxic responses in macrophages (39). Azilsartan, which is a drug currently used to treat hypertension, attenuates oscillatory shear stress-induced endothelial dysfunction and inflammatory responses by upregulating KLF6 (40). However, another study demonstrated that inhibiting KLF6 expression in keratinocytes increases inflammatory responses during aging and accelerates cellular senescence (41). Consequently, different disease models, cell types or stimulation conditions may have a role in the dual effect of KLF6 on inflammatory responses. Nevertheless, few related studies have reported on the role of KLF6 in inflammatory responses. The present study demonstrated that the inflammatory cytokine IL-23 was significantly upregulated in serum samples from patients with ALF, whereas overexpression of KLF6 could reduce the expression of IL-23.

A previous study demonstrated that higher hepatic KLF6 expression is associated with a better prognosis in primary sclerosing cholangitis, which is a chronic liver disease, and KLF6 regulates FXR signaling by binding to FXREs (42). KLF6 can also affect lipid metabolism and activate the mTOR signaling pathway, thereby promoting the progression of renal clear cell carcinoma (43). Nevertheless, the potential mechanisms are insufficiently understood. The present study demonstrated that LPS/GalN-induced ALF was alleviated in antagomir-21 mice. Further study demonstrated that miR-21 promoted the expression of IL-23 by inhibiting KLF6, and KLF6 regulated autophagy. Upregulated IL-23 is associated with inflammatory storms, which have been suggested to be involved in multiple stages of Th17 lineage fate, including in differentiation, expansion and stabilization of Th17 cells (44). TGF-β and IL-6 can induce the expression of retinoic acid-related orphan receptor γt via STAT3 (45), which promote the differentiation of Th17 cells. Upon engagement of IL-23 to its receptor complex, sequential activation of JAK2 and STAT3 occurs (46). Subsequently, cytokines secreted by Th17 cells lead to a combination of inflammatory storms, and subsequent severe hepatocellular necrosis and ALF.

Since the mechanism was determined *in vitro* and may not reflect the actual conditions *in vivo*, further research is needed to expand these findings in mouse models. If reproduced, miR-21 may represent a promising therapeutic strategy for ALF. In conclusion, miR-21 promoted the expression of IL-23 by targeting KLF6, which regulates autophagy, thus promoting inflammatory storms, and subsequent severe hepatocellular necrosis and ALF.

Acknowledgements

Not applicable.

Funding

This study was supported by the Zhejiang Provincial Natural Science Foundation of China (grant no. LQ20H030013), the Zhejiang Province Medical and Health Science and Technology Program (grant no. 2020361785), the National Natural Science Foundation of China (grant no. 82100625), and the Fundamental Research Program Funding of Ninth People's Hospital Affiliated to Shanghai Jiao Tong University School of Medicine (grant no. JYZZ127).

Availability of data and materials

The data generated in the present study may be requested from the corresponding author.

Authors' contributions

SB, WZ and JX contributed to the research design, experimental operation and statistical analysis. RY contributed to the experimental operation and analysis. SB contributed to the manuscript writing and funding. JX and WZ contributed to the critical revision, and helped with the administration and technical support. SB and WZ confirm the authenticity of all the raw data. All authors contributed to the data acquisition and read and approved the final manuscript.

Ethics approval and consent to participate

The research was approved by the Ethics Committee of Zhejiang Provincial People's Hospital, People's Hospital of

Hangzhou Medical College (approval no. for human studies: ZRY-T123-59; approval no. for mice studies: 20190010; Hangzhou, China) Written informed consent was obtained from all participants.

Patient consent for publication

Patients provided written informed consent for publication.

Competing interests

The authors declare that they have no competing interests.

References

1. Tujios S, Stravitz RT and Lee WM: Management of acute liver failure: Update 2022. Semin Liver Dis 42: 362-378, 2022.
2. Bao S, Zheng J, Li N, Huang C, Chen M, Cheng Q, Li Q, Lu Q, Zhu M, Ling Q, *et al*: Role of interleukin-23 in monocyte-derived dendritic cells of HBV-related acute-on-chronic liver failure and its correlation with the severity of liver damage. Clin Res Hepatol Gastroenterol 41: 147-155, 2017.
3. Bao S, Zhao Q, Zheng J, Li N, Huang C, Chen M, Cheng Q, Zhu M, Yu K, Liu C and Shi G: Interleukin-23 mediates the pathogenesis of LPS/GalN-induced liver injury in mice. Int Immunopharmacol 46: 97-104, 2017.
4. Portius D, Sobolewski C and Foti M: MicroRNAs-dependent regulation of PPARs in metabolic diseases and cancers. PPAR Res 2017: 7058424, 2017.
5. Xue Z, Xi Q, Liu H, Guo X, Zhang J, Zhang Z, Li Y, Yang G, Zhou D, Yang H, *et al*: miR-21 promotes NLRP3 inflammasome activation to mediate pyroptosis and endotoxic shock. Cell Death Dis 10: 461, 2019.
6. Hu K, Zheng QK, Ma RJ, Ma C, Sun ZG and Zhang N: Kruppel-like factor 6 splice variant 1: An oncogenic transcription factor involved in the progression of multiple malignant tumors. Front Cell Dev Biol 9: 661731, 2021.
7. Mallipattu SK, Horne SJ, D'Agati V, Narla G, Liu R, Frohman MA, Dickman K, Chen EY, Ma'ayan A, Bialkowska AB, *et al*: Krüppel-like factor 6 regulates mitochondrial function in the kidney. J Clin Invest 125: 1347-1361, 2015.
8. Li J, Yu D, He C, Yu Q, Huo Z, Zhang Y and Zhang S: KLF6 alleviates hepatic ischemia-reperfusion injury by inhibiting autophagy. Cell Death Dis 14: 393, 2023.
9. Sydor S, Manka P, Best J, Jafoui S, Sowa JP, Zoubek ME, Hernandez-Gea V, Cubero FJ, Kälsch J, Vetter D, *et al*: Kruppel-like factor 6 is a transcriptional activator of autophagy in acute liver injury. Sci Rep 7: 8119, 2017.
10. Hu C, Zhao L, Zhang F and Li L: Regulation of autophagy protects against liver injury in liver surgery-induced ischaemia/reperfusion. J Cell Mol Med 25: 9905-9917, 2021.
11. Zhang T, Guo J, Gu J, Chen K, Li H and Wang J: Protective Role of mTOR in liver ischemia/reperfusion injury: Involvement of inflammation and autophagy. Oxid Med Cell Longev 2019: 7861290, 2019.
12. Zeng JJ, Shi HQ, Ren FF, Zhao XS, Chen QY, Wang DJ, Wu LP, Chu MP, Lai TF and Li L: Notoginsenoside R1 protects against myocardial ischemia/reperfusion injury in mice via suppressing TAK1-JNK/p38 signaling. Acta Pharmacol Sin 44: 1366-1379, 2023.
13. Jiang J, Ni L, Zhang X, Wang H, Liu L, Wei M, Li G and Bei Y: Platelet membrane-fused circulating extracellular vesicles protect the heart from ischemia/reperfusion injury. Adv Healthc Mater 12: e2300052, 2023.
14. Chen Y, Wu J, Zhu J, Yang G, Tian J, Zhao Y and Wang Y: Artesunate provides neuroprotection against cerebral ischemia-reperfusion injury via the TLR-4/NF-κB pathway in rats. Biol Pharm Bull 44: 350-356, 2021.
15. Wang Y, Niu H, Li L, Han J, Liu Z, Chu M, Sha X and Zhao J: Anti-CHAC1 exosomes for nose-to-brain delivery of miR-760-3p in cerebral ischemia/reperfusion injury mice inhibiting neuron ferroptosis. J Nanobiotechnology 21: 109, 2023.
16. Hsieh PN, Zhou G, Yuan Y, Zhang R, Prosdocimo DA, Sangwung P, Borton AH, Boriushkin E, Hamik A, Fujioka H, *et al*: A conserved KLF-autophagy pathway modulates nematode lifespan and mammalian age-associated vascular dysfunction. Nat Commun 8: 914, 2017.
17. Guixé-Muntet S, de Mesquita FC, Vila S, Hernández-Gea V, Peralta C, García-Pagán JC, Bosch J and Gracia-Sancho J: Cross-talk between autophagy and KLF2 determines endothelial cell phenotype and microvascular function in acute liver injury. J Hepatol 66: 86-94, 2017.
18. Squires JE, McKiernan P and Squires RH: Acute liver failure: An update. Clin Liver Dis 22: 773-805, 2018.
19. National Research Council (US) Institute for Laboratory Animal Research: Guide for the care and use of laboratory animals. Washington (DC): National Academies Press (US); 1996.
20. Livak KJ and Schmittgen TD: Analysis of relative gene expression data using real-time quantitative PCR and the 2(-Delta Delta C(T)) method. Methods 25: 402-408, 2001.
21. Tong M, Zheng Q, Liu M, Chen L, Lin YH, Tang SG and Zhu YM: 5-methoxytryptophan alleviates liver fibrosis by modulating FOXO3a/miR-21/ATG5 signaling pathway mediated autophagy. Cell Cycle 20: 676-688, 2021.
22. Parrish A, Srivastava A, Juskeviciute E, Hoek JB and Vadigepalli R: Dysregulation of miR-21-associated miRNA regulatory networks by chronic ethanol consumption impairs liver regeneration. Physiol Genomics 53: 546-555, 2021.
23. Rowe MM and Kaestner KH: The role of non-coding RNAs in liver disease, injury, and regeneration. Cells 12: 359, 2023.
24. Lu TX, Munitz A and Rothenberg ME: MicroRNA-21 is up-regulated in allergic airway inflammation and regulates IL-12p35 expression. J Immunol 182: 4994-5002, 2009.
25. Du X, Wu M, Tian D, Zhou J, Wang L and Zhan L: MicroRNA-21 contributes to acute liver injury in LPS-induced sepsis mice by inhibiting PPAR α expression. PPAR Res 2020: 6633022, 2020.
26. Chen X, Song M, Chen W, Dimitrova-Shumkovska J, Zhao Y, Cao Y, Song Y, Yang W, Wang F, Xiang Y and Yang C: MicroRNA-21 contributes to liver regeneration by targeting PTEN. Med Sci Monit 22: 83-91, 2016.
27. Na L, Ding H, Xing E, Zhang Y, Gao J, Liu B, Yu J and Zhao Y: The predictive value of microRNA-21 for sepsis risk and its correlation with disease severity, systemic inflammation, and 28-day mortality in sepsis patients. J Clin Lab Anal 34: e23103, 2020.
28. Liechty C, Hu J, Zhang L, Liechty KW and Xu J: Role of microRNA-21 and its underlying mechanisms in inflammatory responses in diabetic wounds. Int J Mol Sci 21: 3328, 2020.
29. Klionsky DJ, Petroni G, Amaravadi RK, Baehrecke EH, Ballabio A, Boya P, Bravo-San Pedro JM, Cadwell K, Cecconi F, Choi AMK, *et al*: Autophagy in major human diseases. EMBO J 40: e108863, 2021.
30. Klionsky DJ, Abdel-Aziz AK, Abdelfatah S, Abdellatif M, Abdoli A, Abel S, Abeliovich H, Abildgaard MH, Abudu YP, Acevedo-Arozena A, *et al*: Guidelines for the use and interpretation of assays for monitoring autophagy (4th edition)[1]. Autophagy 17: 1-382, 2021.
31. Vargas JNS, Hamasaki M, Kawabata T, Youle RJ and Yoshimori T: The mechanisms and roles of selective autophagy in mammals. Nat Rev Mol Cell Biol 24: 167-185, 2023.
32. Mishra J, Vishwakarma J, Malik R, Gupta K, Pandey R, Maurya SK, Garg A, Shukla M, Chattopadhyay N and Bandyopadhyay S: Hypothyroidism induces interleukin-1-dependent autophagy mechanism as a key mediator of hippocampal neuronal apoptosis and cognitive decline in postnatal rats. Mol Neurobiol 58: 1196-1211, 2021.
33. He WS, Zou MX, Yan YG, Yao NZ, Chen WK, Li Z, Wang WJ and Ouyang ZH: Interleukin-17A promotes human disc degeneration by inhibiting autophagy through the activation of the phosphatidylinositol 3-kinase/Akt/Bcl2 signaling pathway. World Neurosurg 143: e215-e223, 2020.
34. Maneechotesuwan K, Kasetsinsombat K, Wongkajornsilp A and Barnes PJ: Role of autophagy in regulating interleukin-10 and the responses to corticosteroids and statins in asthma. Clin Exp Allergy 51: 1553-1565, 2021.
35. Han D, Huang M, Chang Z and Sun W: KLF15 transcriptionally activates ATG14 to promote autophagy and attenuate damage of ox-LDL-induced HAECs. Mol Biotechnol 66: 112-122, 2024.
36. Zheng Y, Wu J, Chen H, Lin D, Chen H, Zheng J, Xia H, Huang L and Zeng C: KLF4 targets RAB26 and decreases 5-FU resistance through inhibiting autophagy in colon cancer. Cancer Biol Ther 24: 2226353, 2023.
37. Prateeksha P, Naidu P, Das M, Barthels D and Das H: KLF2 regulates neural differentiation of dental pulp-derived stem cells by modulating autophagy and mitophagy. Stem Cell Rev Rep 19: 2886-2900, 2023.

38. Santamaria J, Darrigues J, van Meerwijk JPM and Romagnoli P: Antigen-presenting cells and T-lymphocytes homing to the thymus shape T cell development. Immunol Lett 204: 9-15, 2018.
39. Kim GD, Ng HP, Chan ER and Mahabeleshwar GH: Kruppel-like factor 6 promotes macrophage inflammatory and hypoxia response. FASEB J 34: 3209-3223, 2020.
40. Wei G, Zhu D, Sun Y, Zhang L, Liu X, Li M and Gu J: The protective effects of azilsartan against oscillatory shear stress-induced endothelial dysfunction and inflammation are mediated by KLF6. J Biochem Mol Toxicol 35: 1-8, 2021.
41. Zou Z, Long X, Zhao Q, Zheng Y, Song M, Ma S, Jing Y, Wang S, He Y, Esteban CR, *et al*: A single-cell transcriptomic atlas of human skin aging. Dev Cell 56: 383-397.e8, 2021.
42. Sydor S, Manka P, van Buren L, Theurer S, Schwertheim S, Best J, Heegsma J, Saeed A, Vetter D, Schlattjan M, *et al*: Hepatocyte KLF6 expression affects FXR signalling and the clinical course of primary sclerosing cholangitis. Liver Int 40: 2172-2181, 2020.
43. Syafruddin SE, Rodrigues P, Vojtasova E, Patel SA, Zaini MN, Burge J, Warren AY, Stewart GD, Eisen T, Bihary D, *et al*: A KLF6-driven transcriptional network links lipid homeostasis and tumour growth in renal carcinoma. Nat Commun 10: 1152, 2019.
44. Wu B and Wan Y: Molecular control of pathogenic Th17 cells in autoimmune diseases. Int Immunopharmacol 80: 106187, 2020.
45. Chang D, Xing Q, Su Y, Zhao X, Xu W, Wang X and Dong C: The conserved non-coding sequences CNS6 and CNS9 control cytokine-induced Rorc transcription during T helper 17 cell differentiation. Immunity 53: 614-626.e4, 2020.
46. Abraham C and Cho JH: IL-23 and autoimmunity: New insights into the pathogenesis of inflammatory bowel disease. Annu Rev Med 60: 97-110, 2009.